eJNDT e-Journal of Nondestructive Testing - ISSN 1435-4934 - www.ndt.net

EWSHM 2024
11th European Workshop on Structural Health Monitoring

Concrete crack pixel-level segmentation: a comparison of scene illumination angle of incidence

Hamish DOW[1*], Marcus PERRY[1], Jack MCALORUM[1], Sanjeetha PENNADA[1]
[1] Civil and Environmental Engineering, University of Strathclyde, Glasgow, United Kingdom
[*] hamish.dow@strath.ac.uk

Abstract. Previous research has demonstrated how angled and directional lighting can enhance the detection of concrete cracks in low-light environments and outperform diffused lighting alternatives. This paper investigates the effect of different angles of incidence of directional lighting for concrete crack pixel-level segmentation. Five directional lighting datasets of cracked concrete slabs were captured, each using an angle of incidence of 10, 20, 30, 40, and 50 degrees, respectively. A directional lighting crack segmentation algorithm was applied to each lighting angle dataset. Algorithm output comparisons with ground truths revealed that the directional lighting method performed best on the 50-degree lighting dataset, obtaining a recall, precision, and F1 score of 68%, 81%, and 74%, respectively. However, qualitative analysis of the segmentation outputs on a sub-image scale revealed that towards the edges of the images, the segmentation performance of 30-degree lighting was significantly better, with results closely matching those of the ground truth. This research highlights that the lighting angle of incidence can increase the performance of directional lighting concrete crack segmentation depending on defect position. The results from this work have the potential to improve low-light environment concrete crack detection and monitoring.

Keywords: Image processing, directional lighting, automated inspections, defect detection, binary classification.

Introduction

The majority of concrete structures in Europe, the US, and Asia are now approaching the end of their 50-year lifespan [1]. Early crack identification is crucial to extend the operational lifespan of concrete assets and ensure their safety [2]. However, current manual visual inspection methods are inconsistent, labour-intensive, and pose risks to human physical and mental health [3]. Remote visual inspections using cameras mounted to unmanned vehicles allow safe data acquisition, but manual review of data remains time-consuming and suffers from similar inconsistency issues [4]. In response to these limitations, automated image defect recognition has emerged through transparent image processing methods (white-box techniques) and neural network approaches (black-box techniques) [5]. External lighting is

Media and Publishing Partner
https://doi.org/10.58286/29683

required in low-light environments to illuminate the image scene and make defects visible for white- and black-box methods.

Recent research has shown how projecting angled and directional lighting can provide scene illumination and enhance the detection of concrete cracks in inspection images. Recent studies have also demonstrated how white- and black-box crack detection approaches can provide more accurate and precise crack classification and segmentation results when using directional lighting compared to regular diffused lighting [6], [7]. However, all previous studies have overlooked the effects of the angle of incidence of the projected directional lighting. This paper quantitatively and qualitatively compares the results of a directional lighting pixel-level segmentation white-box method with lighting projected from angles of incidence of 10, 20, 30, 40, and 50 degrees.

1. Directional Lighting Algorithm

A detailed description of the white-box directional lighting algorithm used in this paper is outlined in [6], [7]. A brief explanation is provided below (see Figure 1 for illustration). The algorithm's output shows the extremities of the crack in all lighting directions.

I. **Image acquisition:** four images of the concrete surface are captured, each illuminated with angled lighting projected from the Above (A), Below (B), Right (R), and Left (L) directions. An additional Diffuse lighting (D) image is also captured.
II. **Crack detection:** A 3 × 3 Laplacian kernel is individually applied to each directional lighting image to extract the edges (cracks) using the pre- and post-processing methods outlined by Dorafshan et al. [8].
III. **Image combination & de-noising:** The edge images are combined using a bitwise OR operation, where a resulting pixel is labelled as positive if that pixel is positive in any of the input images. Finally, the skele-marker noise removal method (outlined in [9]) is applied to remove false positive pixels.

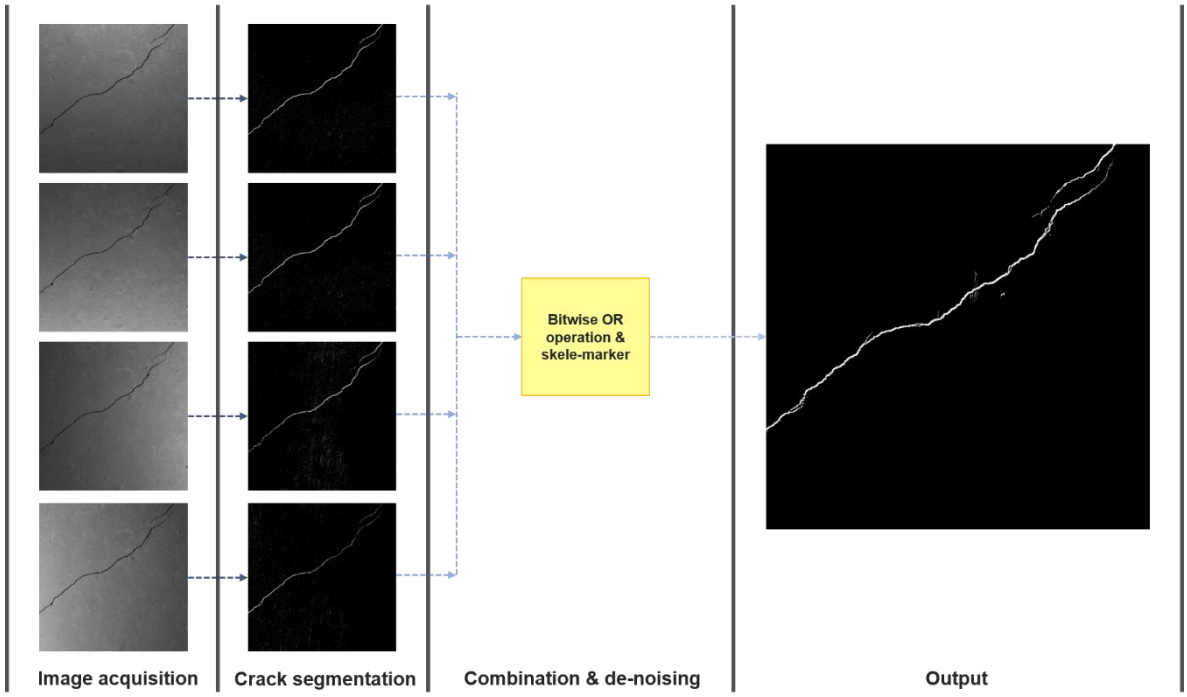

Figure 1. Illustration of directional lighting algorithm used in this paper. A full summary is provided in [6], [7]. The thick crack slab in this figure is indicative and for reader viewing only; it is not used in the analysis.

2. Methodology

2.1 Dataset Formation

Twelve concrete slabs were cast, each featuring varying textures, colours, and imperfections to simulate real-world conditions (see Figure 2a-e). The slabs were fractured with hairline cracks by placing a metal bar behind the slab and applying force to either side. All twelve slabs exhibited crack widths between 0.07 mm and 0.3 mm, well within the 0.4 mm maximum tolerable width for reinforced concrete structures outlined in Eurocode 2 [10].

Each slab was imaged under directional lighting conditions using an iteration of a novel directional lighting apparatus, Adaptive Lighting for the Inspection of Concrete Structures (ALICS). The exact hardware specifications of the device (e.g. camera, working distance, lighting) are outlined in [6].

Five datasets were formed for this study, each using a directional lighting angle of incidence of 10, 20, 30, 40 or 50 degrees, respectively (see Figure 2. a) – e) ample of right lighting with varying angles of incidence.). For each slab in the dataset, five images were captured, matching the A, B, L, R, and D requirements of the directional lighting algorithm. Figure 1 illustrates the different lighting directions subjected to one imaged slab. A total of 300 images were captured for this study, formed from five datasets, each with 12 slabs and five images per slab.

Figure 2 shows an imaged concrete slab from the dataset illuminated with right lighting across all five angled lighting datasets (10, 20, 30, 40 and 50 degrees).

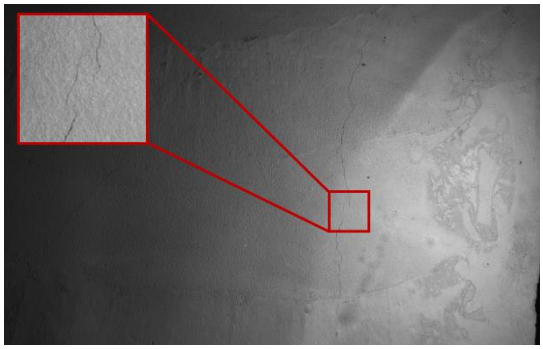

a) 50-degree

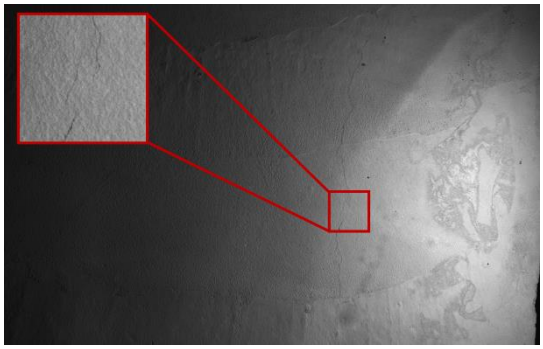

b) 40-degree

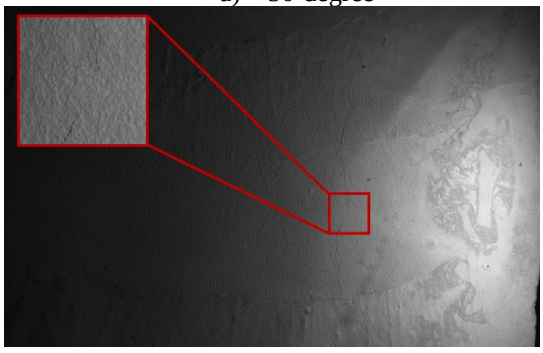

c) 30-degree

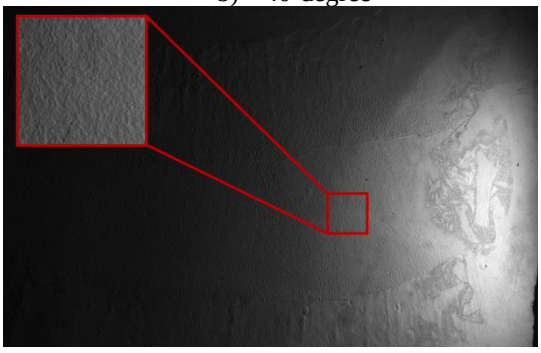

d) 20-degree

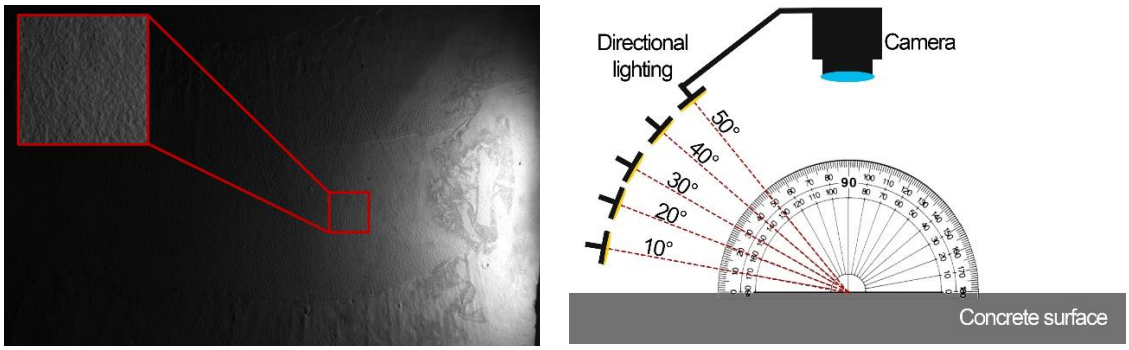

e) 10-degree f) Cross-section of different acquisition angles.

Figure 2. a) – e) ample of right lighting with varying angles of incidence. f) cross-sectional view of lighting apparatus and angles used in this study.

2.2 Ground Truth Definition

Ground truths were defined by manually outlining the crack in image editing software. The width of the tracing tool was adjusted to match the crack width. One ground truth was defined for each slab. As the camera position was fixed during image acquisition, each slab's ground truth was suitable for all five lighting angle datasets.

2.3 Testing Procedure

The directional lighting crack segmentation algorithm was applied to every slab in each lighting angle dataset. This resulted in 12 outputs per lighting angle; each output was compared to their respective ground truth to find the true positives (TP), false negatives (FN), false positives (FP) and true negatives (TN). These values were summed for each dataset, resulting in TP, FN, FP and TN values for every lighting angle. The metrics in Table 1 were calculated to evaluate the performance of each lighting angle.

Table 1. Performance metrics for a classifier.

Name	Description	Equation
True positive rate (recall) (TPR)	The estimated probability that an actual positive will test positive.	$TPR = \frac{TP}{TP + FN}$
Positive predictive value (precisions) (PPV)	The estimated probability that a positive prediction is a true positive.	$PPV = \frac{TP}{TP + FP}$
F1 score (F1)	The weighted average of recall and precision.	$F1 = 2 \times \frac{TPR \times PPV}{TPR + PPV}$

3. Results

3.1 Quantitative Results

Table 2 presents the algorithm's results on each angled lighting dataset, showing TN, TP, FN, and TP compared to the ground truths. Figure 3 shows the algorithm's performance metrics (outlined in Table 1) for each lighting angle of incidence.

Table 2. TN, TP, FN, and TP results of the directional lighting method for each angle of incidence dataset.

Angle (degrees)	TN	FP	FN	TP
50	180,384,252	33,858	68,669	146,821
40	180,325,062	42,547	134,069	131,922
30	180,297,628	81,638	168,835	85,499
20	180,248,259	158,653	187,951	38,737
10	180,039,737	380,458	193,261	20,144

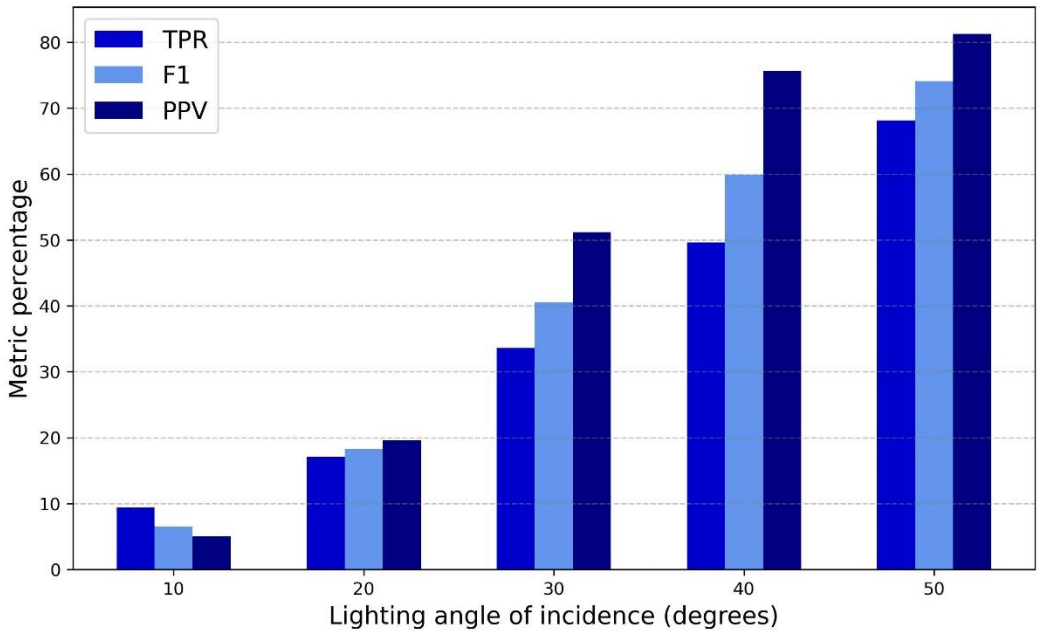

Figure 3. TPR, F1, and PPV values of the directional lighting method for each lighting angle of incidence dataset. Acronyms are described in Table 1.

The directional lighting algorithm achieved the best performance results on the 50-degree lighting dataset, obtaining a recall, precision, and F1 score of 68%, 81%, and 74%, respectively. The 30- and 40-degree lighting datasets had a significant drop in recall when compared to 50-degree lighting. With the exception of 10-degree lighting, all datasets had a higher precision than recall, indicating minimal noise. The performance of 20- and 10-degree lighting was very poor, with all metrics measuring under 20%.

The 50-degree lighting F1 score of 68% is lower than the measured value of 78% from the previous study in [7], likely attributed to noise induced by the real-world simulated dataset. However, the measured F1 value in this study is still greater than the F1 score of 11% from a similar Laplacian-based segmentation method using diffused lighting data tested by Dorafshan et al. [8].

3.2 Qualitative Results

The metrics from the analysis in section 3.1 indicate that 50-degree lighting performs better overall than 30-degree lighting. However, a qualitative analysis provides further insights. Figure 4 shows the algorithm output of one slab using the 50-degree lighting dataset, and Figure 5 shows equivalent output from the 30-degree lighting dataset. Ground truths for both sections are shown in Figure 6.

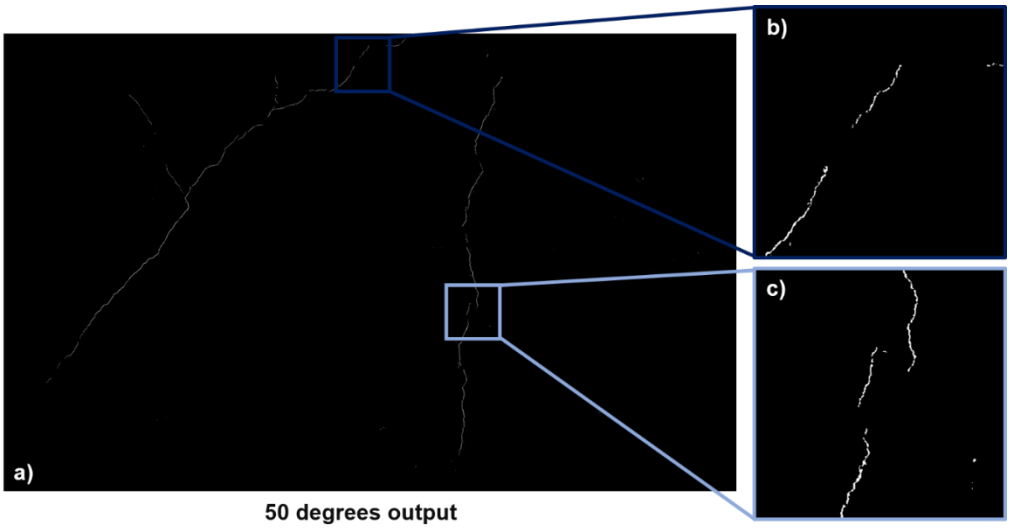

Figure 4. a) output of directional lighting algorithm using 50 degrees lighting, b) inset of an area at the top of the image, c) inset of an area at the middle of the image.

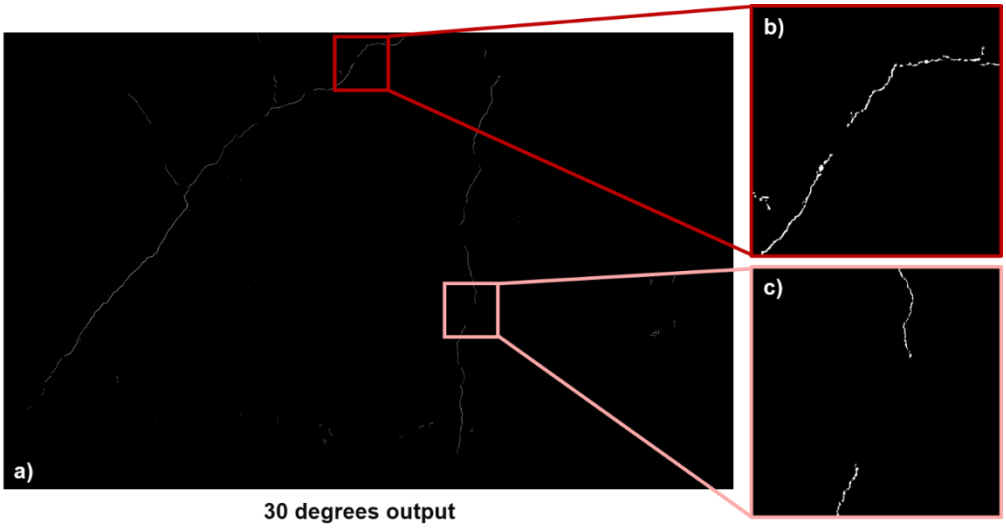

Figure 5. a) output of directional lighting algorithm using 30 degrees lighting, b) inset of an area at the top of the image, c) inset of an area at the middle of the image.

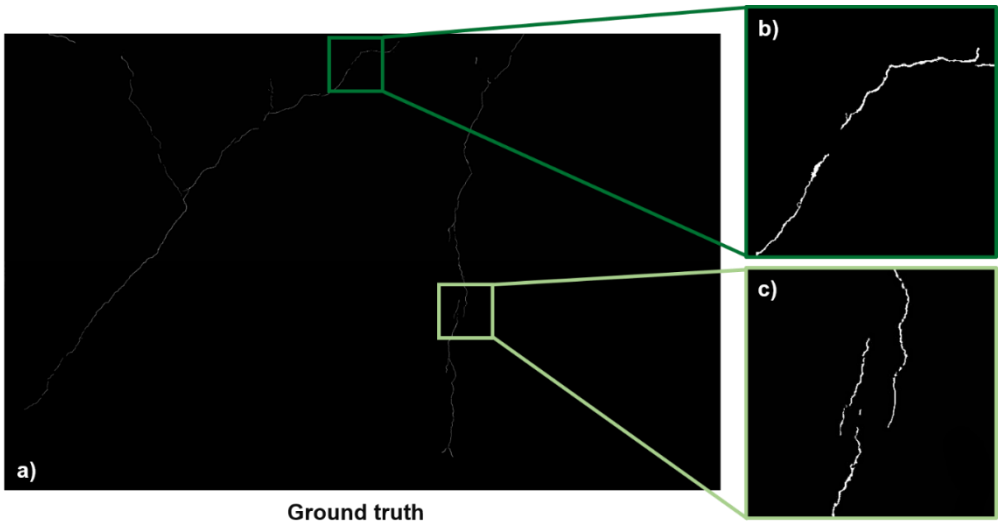

Figure 6. a) Ground truth of dataset samples shown in Figure 4 and Figure 5, b) inset of an area at the top of the image, c) inset of an area at the middle of the image.

Figure 4b and Figure 5b shows the segmentation results for a portion of the slab (towards the edge of the image) for lighting projected from 50 and 30 degrees, respectively. In this sub-image, 30-degree lighting showed better segmentation of the crack when compared to 50-degree lighting, with results closely matching those of the ground truth in Figure 6b.

Figure 4c and Figure 5c illustrates the segmentation results of a sub-image located near the centre of the slab for 50- and 30-degree lighting. In this sub-image, 50-degree lighting has better segmented the crack in comparison to 30-degree lighting, demonstrating a close match to the ground truth in Figure 6c.

4. Conclusion

This paper compared the performance of a directional lighting concrete crack pixel-level segmentation algorithm under different lighting angles of incidence. The tested directional lighting algorithm (proposed in a previous publication) applies crack detection image processing techniques to multiple images of a concrete surface, each illuminated from a different direction. The results from all lighting directions are combined using a bitwise OR operation and de-noised using the skele-marker method. This research compared the performance of the algorithm under 10-, 20-, 30-, 40- and 50-degree angle of incidence lighting on a dataset of 12 cracked concrete slabs. Quantitative analysis showed that 50-degree lighting performed the strongest, obtaining a recall, precision, and F1 score of 68%, 81%, and 74%, respectively. However, qualitative analysis revealed that on a sub-image scale, 50-degree lighting was outperformed by 30-degree lighting towards the edges of the images. In these areas, 30-degree correctly segmented cracks that 50-degree lighting missed entirely. The opposite was true for cracks at the centre of the image, with 50-degree lighting yielding better results than 30-degree. This study has demonstrated that directional lighting crack segmentation results are sensitive to the lighting angle of incidence and defect position. Future studies should investigate combining the segmentation results of different lighting directions: utilising lower-degree angles of lighting at the edges of the images and higher-degree angles of lighting at the centre of the images. Future research should also explore why 30 degrees performs better at the image edges and consider lighting angles above 50 degrees.

References

[1] J. A. Olsson, S. A. Miller, and M. G. Alexander, “Near-term pathways for decarbonizing global concrete production,” *Nat. Commun.*, vol. 14, no. 1, p. 4574, Jul. 2023, doi: 10.1038/s41467-023-40302-0.

[2] Z. Qi, D. Liu, J. Zhang, and J. Chen, “Micro-concrete crack detection of underwater structures based on convolutional neural network,” *Mach. Vis. Appl.*, vol. 33, no. 5, p. 74, Aug. 2022, doi: 10.1007/s00138-022-01327-5.

[3] A. K. Agrawal, G. Washer, S. Alampalli, X. Gong, and R. Cao, “Evaluation of the consistency of bridge inspection quality in New York State,” *J. Civ. Struct. Health Monit.*, vol. 11, no. 5, pp. 1393–1413, Nov. 2021, doi: 10.1007/s13349-021-00517-5.

[4] S. Dorafshan and M. Maguire, “Bridge inspection: human performance, unmanned aerial systems and automation,” *J. Civ. Struct. Health Monit.*, vol. 8, no. 3, pp. 443–476, Jul. 2018, doi: 10.1007/s13349-018-0285-4.

[5] O. Loyola-González, “Black-Box vs. White-Box: Understanding Their Advantages and Weaknesses From a Practical Point of View,” *IEEE Access*, vol. 7, pp. 154096–154113, 2019, doi: 10.1109/ACCESS.2019.2949286.

[6] J. McAlorum, H. Dow, S. Pennada, M. Perry, and G. Dobie, “Automated Concrete Crack Inspection With Directional Lighting Platform,” *IEEE Sens. Lett.*, vol. 7, no. 11, pp. 1–4, Nov. 2023, doi: 10.1109/LSENS.2023.3327611.

[7] H. Dow, M. Perry, J. McAlorum, S. Pennada, and G. Dobie, “A novel directional lighting algorithm for concrete crack pixel-level segmentation,” in *Sensors and Smart Structures Technologies for Civil, Mechanical, and Aerospace Systems 2023*, SPIE, Apr. 2023, pp. 344–350. doi: 10.1117/12.2657235.
[8] S. Dorafshan, R. J. Thomas, and M. Maguire, “Comparison of deep convolutional neural networks and edge detectors for image-based crack detection in concrete,” *Constr. Build. Mater.*, vol. 186, pp. 1031–1045, Oct. 2018, doi: 10.1016/j.conbuildmat.2018.08.011.
[9] H. Dow, M. Perry, J. McAlorum, S. Pennada, and G. Dobie, “Skeleton-based noise removal algorithm for binary concrete crack image segmentation,” *Autom. Constr.*, vol. 151, p. 104867, Jul. 2023, doi: 10.1016/j.autcon.2023.104867.
[10] Eurocode, *Eurocode 2: Design of concrete structures - Part 1-1 : General rules and rules for buildings*. Europe: European Standards, 2004.